Available online at www.sciencedirect.com
ScienceDirect
Journal of Magnetic Resonance 188 (2007) 41–48
JMR Journal of Magnetic Resonance
www.elsevier.com/locate/jmr

High-resolution heteronuclear correlation spectroscopy in solid state NMR of aligned samples

Riqiang Fu [a,*], Milton Truong [b], Randy J. Saager [c], Myriam Cotten [c], Timothy A. Cross [a,b]

[a] Center for Interdisciplinary Magnetic Resonance, National High Magnetic Field Laboratory, 1800 E. Paul Dirac Drive, Tallahassee, FL 32310, USA
[b] Department of Chemistry & Biochemistry, Florida State University, Tallahassee, FL 32306, USA
[c] Department of Chemistry, Pacific Lutheran University, 1010 122d Street South, Tacoma, WA 98447, USA

Received 23 January 2007; revised 12 June 2007
Available online 22 June 2007

Abstract

A new two-dimensional scheme is proposed for accurate measurements of high-resolution chemical shifts and heteronuclear dipolar couplings in NMR of aligned samples. Both the ^{1}H chemical shifts and the ^{1}H–^{15}N dipolar couplings are evolved in the indirect dimension while the ^{15}N chemical shifts are detected. This heteronuclear correlation (HETCOR) spectroscopy yields high-resolution ^{1}H chemical shifts split by the ^{1}H–^{15}N dipolar couplings in the indirect dimension and the ^{15}N chemical shifts in the observed dimension. The advantages of the HETCOR technique are illustrated for a static ^{15}*N*-acetyl-valine crystal sample and a ^{15}N-labeled helical peptide sample aligned in hydrated lipid bilayers.

Keywords: PISEMA; Dipolar coupling; Aligned sample; HETCOR; MSHOT; Solid state NMR

1. Introduction

High-resolution orientational restraints, derived from observations of a wide range of anisotropic nuclear spin interactions such as chemical shifts, homo- and heteronuclear dipolar interactions, and quadrupolar interactions, have been widely used for protein and peptide structural elucidations from aligned samples that have a unique orientation with respect to the magnetic field axis, such as membrane-bound proteins oriented in a hydrated lamellar phase lipid environment [1–9]. In such aligned systems, the data from orientation-dependent nuclear spin interactions within a peptide plane permit the characterization of the peptide plane orientation with respect to the alignment axis. By obtaining the orientations of all peptide planes with respect to the same alignment axis, three-dimensional backbone conformation and topology of the aligned samples can be achieved. Polarization inversion spin exchange at the magic angle (PISEMA) [10], which correlates the orientation-dependent, anisotropic ^{1}H–^{15}N heteronuclear dipolar couplings and ^{15}N chemical shifts, has become a powerful tool to obtain the orientations of peptide planes with respect to the magnetic field axis. In particular, the resonance patterns in the PISEMA spectra of uniformly labeled membrane proteins either mechanically aligned on glass plates or magnetically aligned bicelles form PISA wheels (polarity index slant angle) [11,12], which uniquely defines the helix axis tilt with respect to the alignment axis. However, the anisotropic ^{1}H chemical shift interactions, which provide complementary information, such as the hydrogen bonding geometry [13–16] for the peptide planes, can not be obtained from the PISEMA experiments. In this regard, time-consuming three-dimensional experiments are typically used for measuring the anisotropic ^{1}H chemical shifts [14,15].

With a frequency-switched Lee-Goldburg (FSLG) sequence [17] to suppress proton homonuclear dipolar interactions during the spin exchange period, PISEMA has dramatically improved the resolution of the anisotropic heteronuclear ^{1}H–^{15}N dipolar coupling and ^{15}N chemical

* Corresponding author. Fax: +1 850 644 1366.
E-mail address: rfu@magnet.fsu.edu (R. Fu).

1090-7807/$ - see front matter
doi:10.1016/j.jmr.2007.06.004

shift correlation spectra. However, the performance of the PISEMA experiments largely depends on the FSLG decoupling efficiency, which is very sensitive to the setting of ^{1}H carrier frequencies. In the first half of the FSLG unit (+LG), the ^{1}H radio-frequency (RF) field, $+B_{1H}$, is applied to an offset above a ^{1}H resonance frequency ($+\Delta\omega_H$). In the second half of the FSLG unit (−LG), the opposite ^{1}H RF field, $-B_{1H}$, is applied to the offset below the ^{1}H resonance frequency ($-\Delta\omega_H$). Spin-locking along the magic angle, θ_M, is achieved by setting the RF amplitude and offset to fulfill $\theta_M = \tan(B_{1H}/\Delta\omega_H)$. Under such an ideal condition, the +LG effective field is exactly opposite to the −LG effective field so that the high-order terms in the average Hamiltonian of the FSLG sequence are suppressed [17]. However, in the presence of a ^{1}H resonance offset, Δ, the direction of the +LG effective field is $\theta_+ = \tan\ [B_{1H}/(\Delta\omega_H + \Delta)]$, while the direction of the −LG effective field becomes $\theta_- = \tan[-B_{1H}/(-\Delta\omega_H + \Delta)]$. Obviously, the +LG and +LG effective fields *do not* lie along lines of opposite direction any more. As a result, the high-order terms can no longer be sufficiently suppressed in the average Hamiltonian of the FSLG sequence. For a uniformly labeled protein in which there is a wide range of ^{1}H resonance frequencies due to their anisotropic chemical shifts, especially at high fields, where much-needed sensitivity and chemical shift resolution can be greatly improved, it is simply impossible to satisfy the ideal FSLG condition for all resonances simultaneously. In the PISEMA spectra, such ^{1}H offset effects greatly broaden and thus attenuate the dipolar oscillation peaks in the dipolar dimension of the PISEMA spectra, increase unwanted artifact intensities at zero-frequency of the dipolar dimension, and result in experimental ^{1}H–^{15}N dipolar couplings larger than what they should be.

Many new spectroscopic methods have been proposed to address these problems arising from the ^{1}H offset effects. Recently, π pulses were introduced between the FSLG units to refocus the ^{1}H chemical shift dispersion in the Broadband-PISEMA (BB-PISEMA) experiments [18,19]. However, the π pulse width used has to be very short in order to maintain sufficient FSLG decoupling, especially in strongly coupled spin systems. Alternatively, the SAMMY [20] and SAMPI4 [21] sequences were proposed in which the homonuclear decoupling is achieved by on-resonance pulses using the principle of magic sandwiches. However, due to their long dwell time (7π), compared to (4π) as in the PISEMA experiments, relatively high power ^{1}H RF pulses are required in the dipolar dimension in order to avoid spectral folding in this dimension. Correspondingly, high power ^{15}N RF pulses must be used in order to satisfy the Hartmann–Hahn condition for spin exchange. Use of high power RF pulses is not only technically challenging in probe designs particularly for the low frequency ^{15}N channel with a large rectangular sample coil [22], as typically used to acquire weak NMR signals from aligned samples, but it also results in undesirable sample heating for hydrated biological samples [23]. Recently, Ramamoorthy and co-workers proposed separated local field experiments based on heteronuclear isotropic mixing [24,25], during which the ^{1}H homonuclear dipolar interactions are suppressed and both the ^{1}H and ^{15}N chemical shift anisotropies are refocused by π pulses allowing the scaled ^{15}N–^{1}H dipolar couplings to drive the polarization exchange. Similar to the SAMMY or SAMPI4 experiments, this isotropic mixing also requires the use of high power RF pulses on both the ^{1}H and ^{15}N channels.

In this work, we propose a new scheme in which the magic sandwich high order truncation (MSHOT) homonuclear decoupling sequence [26] is used in the ^{1}H chemical shift (i.e., t_1) dimension, while the ^{15}N chemical shifts are detected (i.e., t_2 dimension) during high power ^{1}H decoupling. This high-resolution two-dimensional (2D) heteronuclear correlation (HETCOR) experiment correlates the orientation-dependent, anisotropic ^{1}H chemical shifts and ^{15}N chemical shifts in the presence of ^{15}N decoupling during the t_1 dimension. In the absence of ^{15}N decoupling during the t_1 dimension, the ^{1}H–^{15}N heteronuclear dipolar couplings evolve along with the ^{1}H chemical shifts, resulting in dipolar splittings in the ^{1}H chemical shift dimension. Such dipolar splittings are high-resolution since the local fields produced by dilute spins at the location of abundant spins are selectively detected, as in proton detected local field (PDLF) experiments [27,28]. In this study, the advantages of this new scheme will be demonstrated by using a static ^{15}*N*-acetyl-valine crystal sample and a ^{15}N-labeled helical peptide sample aligned in hydrated lipid bilayers.

2. Experimental

All NMR measurements were carried out on a Bruker Avance 600 NMR spectrometer with Larmor frequencies of 600.13 and 60.82 MHz for ^{1}H and ^{15}N, respectively, using an NHMFL low electrical field PISEMA probe [29] with a rectangular coil dimension of $7.6 \times 5.6 \times 11$ mm. The SPINAL decoupling sequence [30] with the ^{1}H RF amplitude of 62.5 kHz was used in all experiments during ^{15}N detection in the t_2 dimension. ^{15}N and ^{1}H chemical shifts were referenced to the ^{15}N signal and water peak of an aqueous ^{15}N-labeled ammonium sulfate solution (5%, pH 3.1) at 0 and 4.7 ppm, respectively. In all spectra plotted here, the scales in the t_1 dimension were corrected based on the experimentally determined scaling factors.

Fig. 1a shows the basic pulse sequence for PISEMA experiments. After conventional CP, ^{15}N magnetization is enhanced while the ^{1}H magnetization is flipped to the magic angle, followed by the sequence used for polarization inversion spin exchange. In our PISEMA experiments, the ^{15}N RF spin-lock amplitude of 40 kHz used in the CP was determined via the measurement of 180° pulse-length, while the matching ^{1}H RF spin-lock amplitude was calibrated to be 40 kHz experimentally by the measurement of ^{1}H 180° pulse-length via indirect observation of the ^{15}N signals through CP. The CP contact time was 1 ms. In order to maintain the Hartmann–Hahn match condition

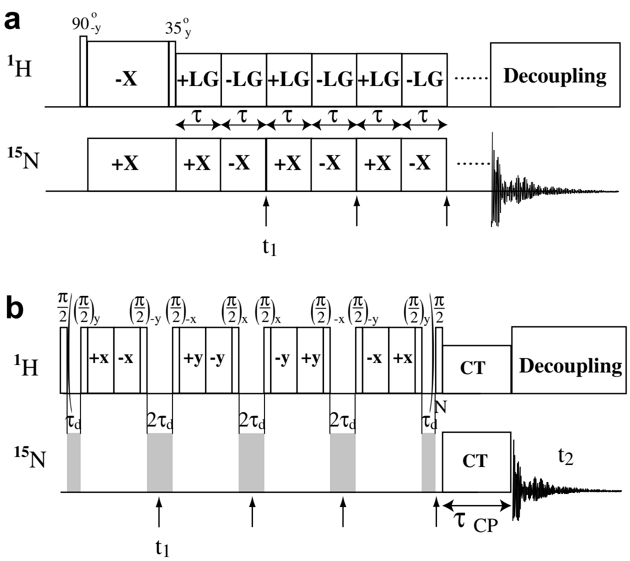

Fig. 1. Pulse sequences for two-dimensional (2D) correlation experiments. (a) PISEMA and (b) HETCOR. The ^{15}N spins are decoupled in the t_1 dimension using a train of grey ^{15}N pulses.

during the spin exchange period, the ^{1}H RF amplitude was decreased to 33 kHz, which was also experimentally calibrated, so that the effective field along the magic angle remained 40 kHz. For each cycle, FSLG was achieved [31] by sweeping the phase of the spin-locking field linearly from 0° to 207.8° for 24.8 μs (+LG) and then from 27.8° to −180° for another 24.8 μs (−LG). Thus the t_1 increment of 49.6 μs generated a dipolar spectral width of 20.16 kHz in the resulting 2D PISEMA spectra. A scaling factor of 0.80 was determined experimentally [31].

Fig. 1b shows the pulse sequence used for our ^{1}H–^{15}N HETCOR experiments. In the t_1 dimension, the MSHOT sequence [26], consisting of basic magic sandwich units with four-step phase cyclings, is applied to suppress the proton homonuclear interactions. A ^{1}H 90° pulse at the end of the t_1 dimension selects the quadrature components using the States phase cycling in the t_1 dimension, followed by a short cross-polarization contact time, τ_{CP}, to ensure that the ^{15}N magnetization is the result of transfer from its closest ^{1}H. In the absence of ^{15}N pulses in the t_1 dimension, both the ^{1}H chemical shifts and the ^{1}H–^{15}N dipolar couplings are evolved, resulting in the ^{1}H–^{15}N dipolar splittings in the ^{1}H chemical shift dimension of the HETCOR spectra. Such dipolar splittings are high-resolution since the ^{1}H local fields produced by ^{15}N are selectively detected via the short CP contact, as in PDLF experiments [27,28]. With a train of grey ^{15}N pulses in the t_1 dimension, the ^{1}H chemical shifts are evolved, leading to typical ^{1}H–^{15}N HETCOR spectra. In our HETCOR experiments, the ^{1}H RF amplitude used for MSHOT decoupling was 62.5 kHz (i.e., 4.0 μs and 16.0 μs for 90° and 360° pulse widths, respectively) and the delay τ_d was 7.0 μs, giving rise to a dwell time of 54.0 μs in the t_1 dimension. The ^{1}H carrier frequency was placed in the center of the ^{1}H chemical shift dimension and no artifacts due to quadrature detection were observed in our spectra. A scaling factor of 0.32 was determined experimentally, which is slightly smaller than the theoretical value [26]. Both the ^{1}H and ^{15}N RF spin-lock fields during CP were 40 kHz and τ_{CP} was 50 μs to transfer the ^{1}H magnetization to its covalently bonded ^{15}N. In fact, in the aligned samples, such a short CP contact time is efficient enough to enhance the ^{15}N signals owing to the rapid buildup of the ^{15}N magnetization in the presence of the dipolar oscillation during CP [32,33], although the rate of the buildup is dependent upon the ^{15}N–^{1}H dipolar coupling. However, in the presence of weak ^{1}H–^{15}N dipolar couplings, there is a need to use more sophisticated CP sequences with a long contact time such as SAMPI4 [21].

3. Results and discussion

Fig. 2 shows the 2D correlation spectra of a static ^{15}*N*-acetyl-valine (NAV) crystal and their representative 1D slices along the t_1 dimension. Two ^{15}N resonances were observed at this arbitrary orientation due to the existence of two magnetically inequivalent molecules per unit cell in the crystal [34]. In these experiments, the ^{1}H carrier frequency was set to the protons that are directly bonded to the ^{15}N peak at 60.8 ppm (i.e., ^{1}H on-resonance decoupling). In the PISEMA spectrum (Fig. 2a), no line-broadening was applied in the t_1 dimension before Fourier transform (FT). From the 1D slice shown in Fig. 2d, the dipolar line-width was 354 Hz and the measured ^{15}N–^{1}H dipolar splitting was 10.8 kHz. A relatively broad dipolar line-width observed here is probably due to the use of a relatively weak ^{1}H RF field in our PISEMA experiments. The truncation of the zero-frequency component leads to the ripple in the spectrum. In the HETCOR spectra (Fig. 2b and c), a Lorentzian line-broadening of 300 Hz was applied in the t_1 dimension before FT. The measured ^{1}H linewidth was 1.6 ppm (i.e., 960 Hz) after compensating for the scaling factor in the ^{1}H chemical shift dimension. Fig. 2b shows the HETCOR spectrum in the absence of ^{15}N decoupling in the ^{1}H chemical shift dimension. Clearly, each of the ^{15}N resonances correlates with a doublet in the ^{1}H chemical shift dimension. The small wiggling at the baseline probably stems from the fact that a single magic sandwich unit was used for the t_1 increment. Theoretically, the MSHOT sequence uses four magic sandwich units for a complete cancellation of up to the 5th high-order term of the ^{1}H homonuclear dipolar interactions [26]. Fig. 2e shows the slice taken at 60.8 ppm along the t_1 dimension, showing a high-resolution doublet with a splitting of 10.8 kHz, which is the same as in Fig. 2d, corresponding to the ^{1}H–^{15}N dipolar coupling. In Fig. 2e, no artifacts were visible in the center of the doublet, while in the PISEMA spectrum artificial intensities at the zero-frequency are typically present. In the presence of ^{15}N decoupling in the ^{1}H chemical shift dimension, each of the doublets collapses into a single resonance in the ^{1}H chemical shift dimension, as shown in Fig. 2c. Fig. 2f shows the slice taken at

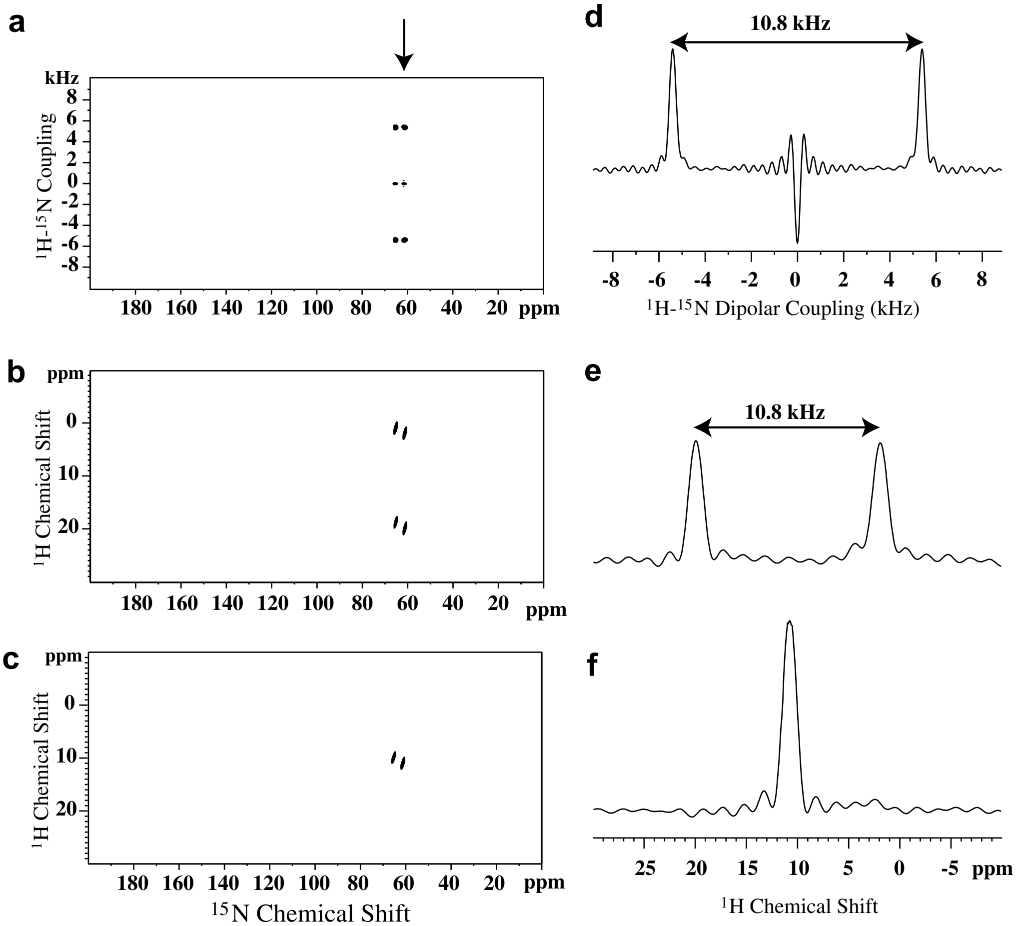

Fig. 2. 2D correlation spectra (left) of a static ^{15}N-acetyl-valine (NAV) crystal at an arbitrary orientation and their one-dimensional (1D) slices taken at 60.8 ppm along the t_1 dimension (marked with an arrow) along the t_1 dimension (right). (a) PISEMA; (b) HETCOR without ^{15}N decoupling during the ^{1}H chemical shift evolution; and (c) HETCOR with ^{15}N decoupling during the ^{1}H chemical shift evolution; (d) an 1D slice taken from (a); (e) an 1D slice taken from (b); and (f) an 1D slice taken from (c). The slices in (b) and (d) show a dipolar splitting of 10.8 kHz. In these 2D experiments, a total of 96 t_1 increments were used and eight scans were used to accumulate signals with a recycle delay of 3 s.

60.8 ppm along the ^{1}H chemical shift dimension, indicating the high-resolution ^{1}H resonance at 10.8 ppm. It can be noticed from Fig. 2e and f that this ^{1}H resonance at 10.8 ppm is positioned in the center of the doublet and its peak intensity is almost twice that of the doublet. In other words, the ^{1}H chemical shift can be extracted by averaging the positions of the peaks in the doublet. Therefore, with no ^{15}N decoupling applied in the ^{1}H chemical shift dimension the HETCOR spectrum allows us to simultaneously obtain the ^{1}H chemical shifts, the ^{1}H–^{15}N dipolar couplings, and ^{15}N chemical shifts, without the need to perform time-consuming three-dimensional experiments [14,15]. Moreover, compared to other techniques such as BB-PISEMA [18,19], SAMMY [20], SAMPI4 [21], and heteronuclear isotropic mixing [24,25], where both high power ^{1}H and ^{15}N RF pulses are used, this new approach does *not* require ^{15}N high power RF pulses for measuring the ^{15}N–^{1}H dipolar couplings. Indeed, the observation of the doublets, rather than the singlets, reduces the sensitivity in half. However, in return, the important ^{1}H chemical shift information becomes available for structural characterization. It is worth noting that the splitting of the resonances into doublets does not necessarily crowd the 2D spectra when the tilt of the helix with respect to the bilayer normal is away from the magic angle. In fact, it forms two asymmetric wheels, instead of one as in PISEMA spectra.

Fig. 3 shows the slices taken at 60.8 ppm, marked with an arrow in Fig. 2, along the t_1 dimension of the PISEMA spectra and the HETCOR spectra without ^{15}N decoupling recorded at different ^{1}H offsets. Obviously, in the PISEMA spectra with the ^{1}H offsets of ±4 kHz, the dipolar linewidth is significantly broadened and the signal intensities are greatly attenuated, which mainly stems from the offset dependence of the homonuclear decoupling efficiency. A larger ^{1}H RF field could decrease this offset effect on the homonuclear decoupling efficiency. On the other hand, the dipolar splitting becomes larger at a given ^{1}H offset (e.g., ±4 kHz) than that observed with the ^{1}H on-resonance condition. This ^{1}H offset dependence of the dipolar splitting has been well demonstrated before [18–21,31] even with a very large ^{1}H RF field [35]. In fact, the ^{1}H offset induces a mismatch between the ^{1}H effective field and the

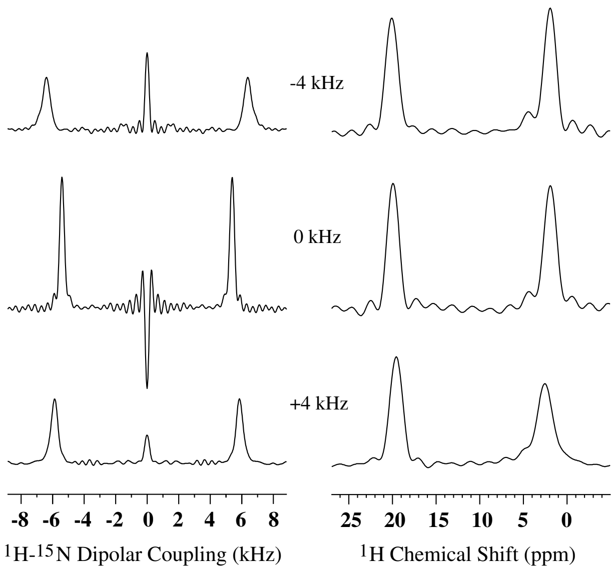

Fig. 3. Slices taken from the ^{15}N resonance at 60.8 ppm, marked with an arrow in Fig. 2, along the t_1 dimension of the PISEMA spectra (left) and the ^{1}H–^{15}N HETCOR spectra without ^{15}N decoupling (right) at different ^{1}H offsets.

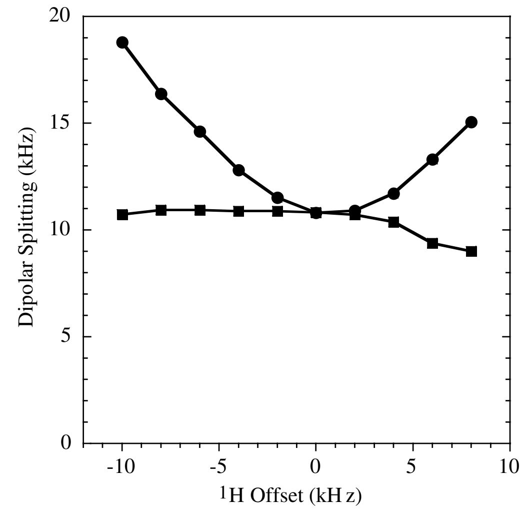

Fig. 4. Dependence of the observed ^{1}H–^{15}N dipolar splitting obtained from the PISEMA spectra (solid circles) and the HETCOR spectra (solid squares) as a function of ^{1}H offset for the peak marked with an arrow in Fig. 2.

^{15}N spin-lock field during the spin exchange period, which results in experimental ^{1}H–^{15}N dipolar couplings larger than what they should be. The ^{1}H offset effect of the dipolar splitting depends not only on the degree of the mismatch but also on the ^{15}N–^{1}H dipolar couplings being studied. In general, such a ^{1}H offset effect is more sensitive to the mismatch when the ^{15}N–^{1}H dipolar coupling is smaller. In contrast, the measured line-width of the ^{1}H resonance at ~20 ppm in the HETCOR spectra was 1.6, 1.6, and 1.7 ppm and the dipolar splitting was 10.9, 10.8, and 10.4 kHz for the ^{1}H offset of −4, 0, and +4 kHz, respectively. Both the dipolar splitting and the intensities of the doublet vary slightly (less than 6%) in the range of the ^{1}H offsets. It is noticeable that the doublet appears not to be symmetric, especially at the ^{1}H offset of +4 kHz, which might stem from the offset dependence of the MSHOT decoupling efficiency. Fig. 4 shows the dependence of the observed dipolar splitting from the PISEMA and HETCOR spectra as a function of ^{1}H offset. Clearly, the dipolar splitting from the HETCOR spectra is less sensitive to the ^{1}H offset in the range of from −10 to +4 kHz compared to the PISEMA spectra. It can be noticed that a relatively weak ^{1}H RF field (33 kHz giving rise to an effective field of 40 kHz) was used in our PISEMA experiments. A stronger ^{1}H RF field should reduce the dependence on the ^{1}H offset effect but can hardly eliminate it [35]. On the other hand, the use of a strong ^{1}H RF field requires a strong ^{15}N RF field to fulfill the spin exchange match condition, which is challenging in terms of NMR probe designs for the low gamma nucleus and large sample coil. In this regards, the advantage of the HETCOR method is significant, since it does not require the ^{15}N RF field for measuring the ^{1}H–^{15}N dipolar couplings.

Piscidins, amphipathic cationic antimicrobial peptides (ACAPs) from the mast cells of fish, are believed to play a crucial and direct role in the fight against many aquatic bacterial infections [36,37]. Two isoforms of these peptides, piscidins 1 and 3 (i.e., p1 and p3) have been structurally analyzed using solid state NMR [38,39]. Here, the amidated ^{15}N-$V_{10}G_{13}I_{16}$p1-NH_2 peptide of amino acid sequence FFHHIFRGIVHVGKTIHRLVTG was chemically synthesized and an hydrated oriented sample was prepared for solid state NMR by using lipid films of 1,2-dimyristoyl-*sn*-glycero-3-phosphatidyl-choline (DMPC) and 1,2-dimyristoyl-*sn*-glycero-3-phospho-rac-(1-glycerol) (DMPG) containing 10 mg of peptide, as detailed previously [39]. Fig. 5 shows the 2D correlation spectra of the ^{15}N-$V_{10}G_{13}I_{16}$p1-NH_2 peptide aligned in hydrated lipids (with a molar peptide to lipid ratio of 1:20 and a DMPC to DMPG molar ratio of 3:1) and their representative 1D slices along the indirect dimension. The ^{1}H carrier frequency was set to 10.8 ppm in these experiments. Three sharp ^{15}N resonances were observed in the spectra at 39.9, 43.7, and 54.0 ppm, having line-widths of 1.7, 1.8, and 2.4 ppm, respectively (with 10 Hz line-broadening). Clearly, the peptide sample is well aligned and its helical axis is almost perpendicular to the magnetic field and the bilayer normal since the observed ^{15}N chemical shifts are close to the perpendicular component of the ^{15}N chemical shift tensor. Based on the measurements from specific labeling samples [39] and simulations of PISA wheels and dipolar waves [40], the ^{15}N resonances at 39.9, 43.7, and 54.0 ppm were tentatively assigned to the I_{16}, G_{13}, and V_{10} label sites, respectively, In the PISEMA spectrum (Fig. 5a), no line-broadening was applied in the t_1 dimension before FT. From the 1D slices, the observed dipolar line-widths were 380, 400, and 510 Hz and the ^{15}N–^{1}H dipolar splitting were 10.2, 8.4, and 9.0 kHz for the I_{16}-, G_{13}-, and V_{10}-labeled sites, respectively.

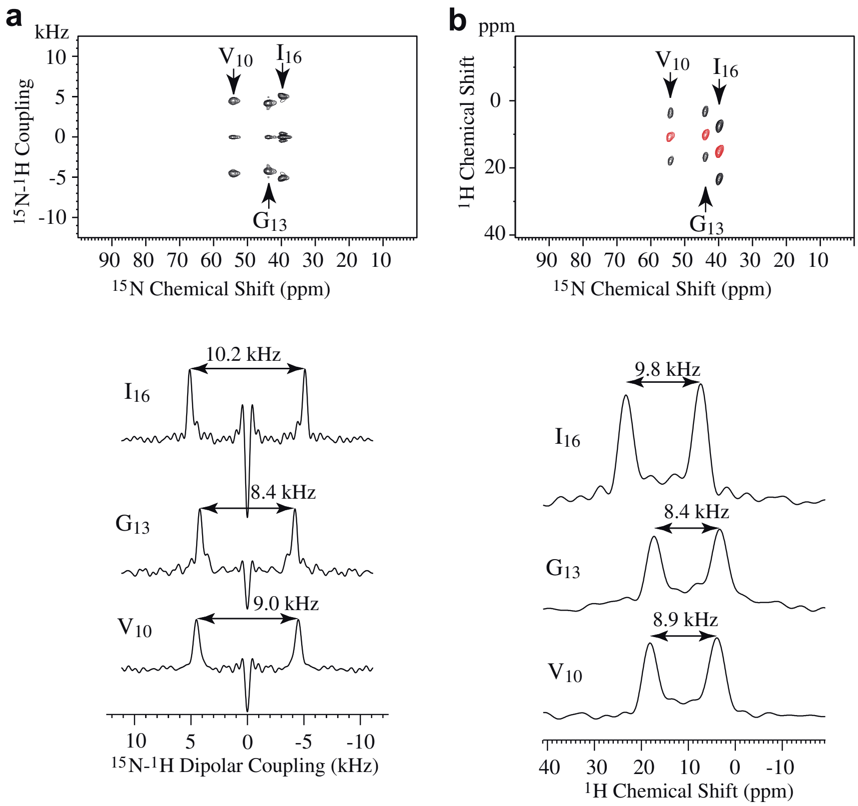

Fig. 5. 2D correlation spectra of ^{15}N-$V_{10}G_{13}I_{16}$p1-NH_2 peptide oriented in lipid bilayers and their 1D slices along the indirect dimension. (a) PISEMA; (b) superimposed HETCOR spectra with (red) and without (black) ^{15}N decoupling in the t_1 dimension. A total of 48 t_1 increments were used in these experiments and 512 scans were used to accumulate the signals with a recycle delay of 4 s.

Fig. 5b shows the superimposed HETCOR spectra of the ^{15}N-$V_{10}G_{13}I_{16}$p1-NH_2 peptide oriented in hydrated lipids with (red) and without (black) ^{15}N decoupling in the t_1 dimension. Below the 2D spectra are representative 1D slices along the indirect dimension of the HETCOR spectrum in the absence of ^{15}N decoupling. In these HETCOR spectra (Fig. 5b), a Lorentzian line-broadening of 1200 Hz (i.e., 2.0 ppm) was applied in the t_1 dimension before FT. Such a large line-broadening used in the processing is mainly for masking the signal truncation in the t_1 dimension, since some signals were still visible after 48 t_1 increments. Fortunately, this truncation does not affect the resolution in the 2D spectra because the three resonances from this sample are well resolved, although the signals in the 1D dipolar slices are significantly broadened. In the presence of ^{15}N decoupling, the HETCOR spectrum showed that the amide ^{1}H chemical shifts are 15.4, 10.4, and 11.3 ppm, having line-widths of 3.3, 3.3, and 3.5 ppm, after compensating for the scaling factor in the ^{1}H chemical shift dimension, for the ^{15}N I_{16}-, G_{13}-, and V_{10}-labeled sites, respectively. Therefore, in these PISEMA and HETCOR experiments, the ^{1}H offsets for the I_{16}, G_{13} and V_{10} sites were 2.76, 0.24, and 0.30 kHz, respectively. In the absence of ^{15}N decoupling, the observed ^{1}H line-widths from the HETCOR spectrum were 3.5, 3.9, and 3.7 ppm, after considering the scaling factor, slightly broader than that obtained from the HETCOR in the presence of ^{15}N decoupling. In addition, the measured ^{15}N–^{1}H dipolar splittings from the HETCOR spectrum were 9.8, 8.4, and 8.9 kHz for the I_{16}-, G_{13}-, and V_{10}-labeled sites, respectively. Clearly, the ^{15}N–^{1}H dipolar splittings for the G_{13} and V_{10} sites generated from the HETCOR spectrum are the same as from the PISEMA spectrum, owing to the fact that the amide protons from these two-labeled sites are almost under on-resonance irradiation conditions. However, the ^{15}N–^{1}H dipolar splitting obtained from the PISEMA spectrum for the I_{16} site is about 400 Hz greater than that from the HETCOR spectrum, due to the ^{1}H offset (e.g., 2.76 kHz) effects in the PISEMA spectra. Therefore, in multiple-site-labeled samples, the HETCOR spectrum in the absence of ^{15}N decoupling not only accurately measures ^{15}N–^{1}H dipolar splittings for all sites, but also provides ^{1}H chemical shifts for the amide protons. Characterization of the p1 structure is a necessary step in the search for relationships between structural motifs, interactions with biological membranes, potency, and mechanisms of action. The PISEMA experiments performed as part of the structural studies [39] and corresponding simulations have indicated that the peptide is α-helical and oriented perpendicular to (~89°) the bilayer normal. The additional ^{1}H chemical shift information obtained here may give new insights about the interactions of the peptide helix with the bilayer and aqueous environments. Detailed studies are currently in progress.

4. Conclusion

We have demonstrated that two-dimensional high-resolution ^{1}H–^{15}N heteronuclear correlation (HETCOR) spectroscopy provides an efficient means for simultaneously measuring anisotropic ^{1}H–^{15}N dipolar couplings, ^{1}H chemical shifts, and ^{15}N chemical shifts in NMR spectroscopy of aligned samples. Here, the MSHOT homonuclear decoupling sequence [26] is used to suppress the ^{1}H homonuclear dipolar interactions while allowing for the evolution of ^{1}H–^{15}N dipolar couplings and ^{1}H chemical shifts in the indirect dimension. The robust MSHOT sequence is capable of sufficient suppression of the ^{1}H homonuclear interactions even in the presence of substantial ^{1}H offsets and ^{15}N–^{1}H dipolar couplings, which can not be achieved by the FSLG sequence, although the former sequence exhibits a smaller scaling factor than the latter one. It has been shown here that when the ^{1}H RF amplitude is 62.5 kHz, the obtained ^{1}H–^{15}N dipolar splittings and the signal intensities of the HETCOR spectra are not sensitive to the ^{1}H carrier frequency in a bandwidth of at least 14 kHz. It is anticipated that the effective ^{1}H bandwidth for the HETCOR spectra should increase with an increase of the ^{1}H RF amplitude. Thus, this new approach provides significant additions to other recently developed techniques [18–21,24,25] in terms of minimizing the ^{1}H offset effects as well as obtaining anisotropic ^{1}H chemical shift information. With a large effective ^{1}H bandwidth, this approach will be particularly useful at higher fields where the anisotropy of the diamagnetic or paramagnetic susceptibility can aid sample alignment thus enhancing both the ^{1}H and ^{15}N resolution. More importantly, this HETCOR scheme proposed here *does not* require high power ^{15}N pulses, which further minimizes the RF heating of hydrated samples and reduces the specifications for the RF probes. Potentially, such a HETCOR scheme can be converted into a ^{1}H-detected HETCOR scheme, which may significantly enhance the sensitivity. It is expected that the HETCOR scheme will become valuable in the structural studies of aligned samples such as membrane proteins oriented in hydrated lipid bilayers.

Acknowledgments

This work was supported in part by the NSF MCB 02-35774 (T.A.C. and R.F.) and performed largely at the National High Magnetic Field Laboratory supported by the NSF Cooperative Agreement DMR-0084173 and the State of Florida. M.C. and R.J.S. are grateful for support from Research Corporation, the Dreyfus Foundation, and the Undergraduate Research Summer program at Pacific Lutheran University. The authors thank Dr. Nevzorov from Prof. Opella's group at the Center for NMR Spectroscopy and Imaging of Proteins (University of California San Diego) for the simulations of dipolar waves for piscidin 1.

References

[1] R.R. Ketchem, B. Roux, T.A. Cross, High-resolution polypeptide structure in a lameller phase lipid environment from solid state NMR derived orientational constraints, Structure 5 (1997) 1655–1669.

[2] Y. Kim, K. Valentine, S.J. Opella, S.L. Schendel, W.A. Cramer, Solid-state NMR studies of the membrane-bound closed state of the colicin e1 channel domain in lipid bilayers, Protein Sci. 7 (1998) 342–348.

[3] Z. Song, F. Kovacs, J. Wang, J. Denny, S.C. Shekar, J.R. Quine, T.A. Cross, Transmembrane domain of M2 protein from Influenza A virus studied by solid-state ^{15}N polarization inversion spin exchange at magic angle NMR, Biophys. J. 79 (2000) 767–775.

[4] K. Nishimura, S. Kim, L. Zhang, T.A. Cross, The closed state of a H^+ channel helical bundle combining precise orientational and distance restraints from solid state NMR, Biochemistry 41 (2002) 13170–13177.

[5] F.M. Marassi, S.J. Opella, Simultaneous assignment and structure determination of a membrane protein from NMR orientational restraints, Protein Sci. 12 (2003) 403–411.

[6] A.A. DeAngelis, S.C. Howell, A.A. Nevzorov, S.J. Opella, Structure determination of a membrane protein with two transmembrane helices in aligned phospholipid bicelles by solid-state NMR spectroscopy, J. Am. Chem. Soc. 128 (2006) 12256–12257.

[7] A.A. DeAngelis, A.A. Nevzorov, S.H. Park, S.C. Howell, A.A. Mrse, S.J. Opella, High-resolution NMR spectroscopy of membrane proteins in "Unflipped" bicelles, J. Am. Chem. Soc. 126 (2004) 15340–15341.

[8] A. Ramamoorthy, Y. Wei, D.K. Lee, PISEMA solid-state NMR spectroscopy, Annu. Rep. NMR Scpectroscopy 52 (2004) 1–52.

[9] T. Vosegaard, N.C. Nielsen, Towards high-resolution solid-state NMR on large uniformly ^{15}N- and [^{13}C, ^{15}N]-labeled membrane proteins in oriented lipid bilayers, J. Biomol. NMR 22 (2002) 225–247.

[10] C.H. Wu, A. Ramamoorthy, S.J. Opella, High-resolution heteronuclear dipolar solid-state NMR spectroscopy, J. Magn. Reson. Ser. A 109 (1994) 270–272.

[11] F.M. Marassi, S.J. Opella, A solid-state NMR index of helical membrane proteins structure and topology, J. Magn. Reson. 144 (2000) 150–155.

[12] J. Wang, J. Denny, C. Tian, S. Kim, Y. Mo, F. Kovacs, Z. Song, K. Nishimura, Z. Gan, R. Fu, J.R. Quine, T.A. Cross, Imaging membrane protein helical wheels, J. Magn. Reson. 144 (2000) 162–167.

[13] C.H. Wu, A. Ramamoorthy, L.M. Gierasch, S.J. Opella, Simultaneous characterization of the amide ^{1}H chemical shift, ^{1}H–^{15}N dipolar, and ^{15}N chemical shift interaction tensors in a peptide bond by three-dimensional solid-state NMR spectroscopy, J. Am. Chem. Soc. 117 (1995) 6148–6149.

[14] A. Ramamoorthy, C.H. Wu, S.J. Opella, Three-dimensional solid-state NMR experiment that correlates the chemical shift and dipolar coupling frequencies of two heteronuclei, J. Magn. Reson. B 107 (1995) 88–90.

[15] R. Jelinek, A. Ramamoorthy, S.J. Opella, High-resolution three-dimensional solid-state NMR spectroscopy of a uniformly ^{15}N-labeled protein, J. Am. Chem. Soc. 117 (1995) 12348–12349.

[16] Y. Wei, D.K. Lee, K.J. Hallock, A. Ramamoorthy, One-dimensional ^{1}H-detected solid state NMR experiment to determine amide-^{1}H chemical shifts in peptides, Chem. Phys. Lett. 351 (2002) 42–46.

[17] A. Bielecki, A.C. Kolbert, H.J.M. de Groot, R.G. Griffin, M.H. Levitt, Frequency-switched Lee-Goldburg sequences in solids, Adv. Magn. Reson. 14 (1990) 111–150.

[18] K. Yamamoto, D.K. Lee, A. Ramamoorthy, Broadband-PISEMA solid state NMR spectroscopy, Chem. Phys. Lett. 407 (2005) 289–293.

[19] S.V. Dvinskikh, D. Sandstrom, Frequency offset refocused PISEMA-type sequences, J. Magn. Reson. 175 (2005) 163–169.

[20] A.A. Nevzorov, S.J. Opella, A "Magic Sandwich" pulse sequence with reduced offset dependence for high-resolution separated local field spectroscopy, J. Magn. Reson. 164 (2003) 182–186.

[21] A.A. Nevzorov, S.J. Opella, Selective averaging for high-resolution solid-state NMR spectroscopy of aligned samples, J. Magn. Reson. 185 (2007) 59–70.
[22] P.L. Gor'kov, E.Y. Chekmenev, R. Fu, J. Hu, T.A. Cross, M. Cotten, W.W. Brey, A large volume flat coil probe for oriented membrane proteins, J. Magn. Reson. 181 (2006) 9–20.
[23] C. Li, Y. Mo, J. Hu, E.Y. Chekmenev, C. Tian, F.P. Gao, R. Fu, P.L. Gor'kov, W.W. Brey, T.A. Cross, Analysis of RF heating and sample stability in aligned static solid state NMR spectroscopy, J. Magn. Reson. 180 (2006) 51–57.
[24] K. Yamamoto, S.V. Dvinskikh, A. Ramamoorthy, Measurement of heteronuclear dipolar couplings using a rotating frame solid-state NMR experiment, Chem. Phys. Lett. 419 (2006) 533–536.
[25] S.V. Dvinskikh, K. Yamamoto, A. Ramamoorthy, Heteronuclear isotropic mixing separated local field NMR spectroscopy, J. Chem. Phys. 125 (2006) 034507.
[26] M. Hohwy, N.C. Nielsen, Elimination of high order terms in multiple pulse nuclear magnetic resonance spectroscopy: application to homonuclear decoupling in solids, J. Chem. Phys. 106 (1997) 7571–7586.
[27] K. Schmidt-Rohr, D. Nanz, L. Emsley, A. Pines, NMR measurement of resolved heteronuclear dipole couplings in liquid crystals and lipids, J. Phys. Chem. 98 (1994) 6668–6670.
[28] S.V. Dvinskikh, U. Durr, K. Yamamoto, A. Ramamoorthy, A high-resolution solid state NMR approach for the structural studies of bicelles, J. Am. Chem. Soc. 128 (2006) 6326–6327.
[29] P.L. Gor'kov, E.Y. Chekmenev, C. Li, M. Cotten, J.J. Buffy, N.J. Traaseth, G. Veglia, W.W. Brey, Using low-E resonators to reduce RF heating in biological samples for static solid-state NMR up to 900 MHz, J. Magn. Reson. 185 (2007) 77–93.
[30] B.M. Fung, A.K. Khitrin, K. Ermolaev, Am improved broadband decoupling sequence for liquid crystals and solids, J. Magn. Reson. 142 (2000) 97–101.
[31] R. Fu, C. Tian, H. Kim, S.A. Smith, T.A. Cross, The effect of Hartmann–Hahn mismatching on polarization inversion spin exchange at the magic angle, J. Magn. Reson. 159 (2002) 167–174.
[32] L. Müller, A. Kumar, T. Baumann, R.R. Ernst, Transient oscillations in NMR cross-polarization experiments in solids, Phys. Rev. Lett. 32 (1974) 1402–1406.
[33] F. Tian, T.A. Cross, Dipolar oscillations in cross-polarized peptide samples in oriented lipid bilayers, J. Magn. Reson. 125 (1997) 220–223.
[34] P.J. Carroll, P.L. Stewart, S.J. Opella, Structures of two model peptides: *N*-acetyl-D,L-valine and *N*-acetyl-L-valine-leucine, Acta Cryst. C46 (1990) 243–246.
[35] Z. Gan, Spin dynamics of polarization inversion spin exchange at the magic angle spinning in multiple spin systems, J. Magn. Reson. 143 (2000) 136–143.
[36] U. Silphaduang, E.J. Noga, Peptide antibiotics in mast cells of fish, Nature 414 (2001) 268–269.
[37] X. Lauth, H. Shike, J.C. Burns, M.E. Westerman, V.E. Ostland, J.M. Carlberg, J.C. van Olst, V. Nizet, S.W. Taylor, C. Shimizu, P. Bulet, Discovery and characterization of two isoforms of moronecidin, a novel antimicrobial peptide from hybrid striped bass, J. Biol. Chem. 277 (2002) 5030–5039.
[38] E.Y. Chekmenev, S.M. Jones, Y.N. Nikolayeva, B.S. Vollmar, T.J. Wagner, P.L. Gor'kov, W.W. Brey, M.N. Manion, K.V. Daugherty, M. Cotten, High-field NMR studies of molecular recognition and structure–function relationships in antimicrobial piscidins at the water-lipid bilayer interface, J. Am. Chem. Soc. 128 (2006) 5308–5309.
[39] E.Y. Chekmenev, B.S. Vollmar, K.T. Forseth, M.N. Manion, S.M. Jones, T.J. Wagner, R.M. Endicott, B.P. Kyriss, L.M. Homem, M. Pate, J. He, J. Raines, P.L. Gor'kov, W.W. Brey, D.J. Mitchell, A.J. Auman, M.J. Ellard-Ivey, J. Blazyk, M. Cotten, Investigating molecular recognition and biological function at interfaces using piscidins, antimicrobial peptides from fish, Biochem. Biophys. Acta 1758 (2006) 1359–1372.
[40] S.J. Opella, F.M. Marassi, Structure determination of membrane proteins by NMR spectroscopy, Chem. Rev. 104 (2004) 3587–3606.